CYpHER: Catalytic extracellular targeted protein degradation with high potency and durable effect

Zachary R. Crook[1,2,3], Gregory P. Sevilla[1,2,3], Pamela Young[2], Emily J. Girard[4], Tinh-Doan Phi[2], Monique L. Howard[5], Jason Price[3], James M. Olson[3,4], Natalie W. Nairn[1,2]*.

1-Cyclera Therapeutics Inc, Seattle, WA 98115, USA.

2-Blaze Bioscience Inc, Seattle, WA 98109, USA.

3-Clinical Research Division, Fred Hutchinson Research Center, Seattle, WA 98109, USA.

4-Ben Towne Center for Childhood Cancer Research, Seattle Children's Research Institute, Seattle, WA 98105, USA.

5-NW Biosensor, Seattle, WA 98103, USA.

*Corresponding Author. Email: natalie.nairn@cycleratx.com

Supplementary Methods

Recombinant proteins, antibodies, and co-stains/secondary antibodies.

Recombinant proteins used for surface display flow cytometry and for catalytic uptake of soluble proteins were as follows: biotinylated His-Avi-tagged human PD-L1 ectodomain (ACROBiosystems PD1-H82E5); biotinylated His-Avi-tagged human full-length EGFR ectodomain (VHH nanobody analysis, ACROBiosystems EGR-H82E3); biotinylated His-Avi-tagged human EGFRvIII ectodomain (EGF variant analysis and soluble EGFR uptake, ACROBiosystems EGR-H82E0); biotinylated His-Avi-tagged human TfR (TfR cross-reactivity, ACROBiosystems TFR-H82E5); His-tagged mouse TfR (TfR cross-reactivity, R&D Systems 9706-TR-050; note that this was produced in Chinese hamster ovary [CHO] cells, as opposed to all other recombinant proteins that were produced in human HEK cells).

Primary antibodies for surface protein staining were as follows: EGFR, clone 199.12 (ThermoFisher MA5-13319); TfR, clone OKT9, APC-labeled (ThermoFisher 17-0719-42); PD-L1, clone 22C3 (Agilent M365329-1). Primary antibodies for Western blotting are as follows: rabbit anti-EGFR (Cell Signaling Technology 2646); rabbit anti-phospho-Y1068 EGFR (Cell Signaling Technology 3777); goat anti-actin (Abcam

ab8229). Secondary antibodies or co-stains were as follows: Alexa Fluor 647-conjugated streptavidin (surface display staining other than TfR human/mouse cross-reactivity, ThermoFisher S21374); iFluor 647-conjugated anti-His-tag antibody (pilot CYpHER detection and TfR human/mouse cross-reactivity, Genscript A01802); Alexa Fluor 647-conjugated anti-Fc Fab (Surface protein and CYpHER quantitation, ThermoFisher Zenon Labeling Kits, mouse IgG2a for anti-EGFR 199.12 quantitation [ThermoFisher Z25108], mouse IgG1 for anti-PD-L1 22C3 quantitation [ThermoFisher Z25008], human IgG for CYpHER quantitation [ThermoFisher Z25408]); iFluor 647-conjugated sAvPhire monovalent streptavidin (catalytic soluble protein uptake, Millipore Sigma SAE178-100UG); iFluor 488-conjugated sAvPhire monovalent streptavidin (catalytic soluble protein uptake, Millipore Sigma SAE176-100UG); IRDye 680RD Donkey anti-goat (Western blotting, LI-COR 926-68074); IRDye 800CW Donkey anti-rabbit (Western Blotting, LI-COR 926-32213). Antibodies were validated by vendors, found on product websites by vendor and catalog number.

Cancer cell lines and primary keratinocytes sources

All parental cancer lines, and primary keratinocytes, were sourced from ATCC (A549, CCL-185; H1975, CRL-5908; H1650, CRL-5883; H358, CRL-5807; MDA-MB-231, CRM-HTB-26; SW48, CCL-231; primary keratinocytes, PCS-200-011). A549-EGFR-GFP cells were purchased from Sigma (CLL1141-1VL).

Conversion of EGF into a dominant-negative EGF variant for CYpHER incorporation.

EGF itself was modified to disable signal transduction capabilities. Here, binding to both Domain I and Domain III of EGFR induces a conformational change that renders the dimerization domain (Domain II) solvent-accessible[1]. This facilitates homo- or heterodimerization partner cross-phosphorylation in the cytosolic kinase domains and subsequent signal transduction. Engineering EGF to eliminate Domain I-binding while enhancing Domain III-binding was done to produce a dominant-negative EGF variant, and candidate CYpHER component, that competitively engages EGFR but does not induce Domain II-dependent dimerization and signal transduction.

After using Rosetta protein design software[2-4] to design and screen 488 variants that were predicted to have improved binding to Domain III based on a published co-crystal structure[1], mammalian surface display screening for binding to EGFRvIII produced two variants (Supplementary Fig. 3, A and B) named EGFd1 and

EGFd2; EGFd1 demonstrated the strongest binding in surface display. The EGF:EGFR co-crystal structure[1] was further studied to identify four residues (M21, A30, I38, and W49) on EGF that contact Domain I such that mutations to them would be predicted to disrupt the interface, either eliminating hydrophobic interactions or introducing steric hindrance. Mutations to disrupt these residues one at a time (EGFd1.1 through 1.4), and one that disrupted all four at once (EGFd1.5), were tested for the ability to bind full-length EGFR or EGFRvIII. Three of the four Domain I interface point mutants (EGFd1.1, EGFd1.2, and EGFd1.3) and the quadruple mutant (EGFd1.5) demonstrated improved EGFRvIII binding, while all five EGFd1 variants demonstrated a substantial increase in the ratio of EGFRvIII binding vs full-length EGFR binding, indicating an apparent negative contribution of Domain I to EGFR binding (Supplementary Fig. 3C). Advancing EGFd1.5, it demonstrated a reduced stain in mammalian surface display upon pH 5.5 rinse, similar to that seen for EGFR Nanobody v1 (Supplementary Fig. 3D); as EGF is known to naturally possess pH-dependent EGFR binding[5], this EGFd1.5 behavior confirmed the engineered variant retained this property. An additional round of affinity maturation (site-saturation mutagenesis followed by pooled mammalian display enrichment screening over two rounds of sorting)[6] yielded a higher-affinity variant (Supplementary Fig. 3E), EGFd1.5.36, that was chosen for testing in the CYpHER context.

Mammalian surface display

293F cells (ThermoFisher R79007) were grown in FreeStyle 293 expression medium (ThermoFisher 12338018) in 37°C, 8% CO_2 humidified shaking incubators. Proteins were surface displayed via transient transfection (singleton testing) or lentiviral transduction (pooled screening) using vector SDGF[7], in which displayed proteins have a free C-terminus, or a variant thereof where the displayed protein has a free N-terminus and is connected to C-terminal GFP by a Type 1 transmembrane domain derived from human CD28. The parental C-terminal display vector was used for experiments involving CDPs (including EGF and variants thereof), while the N-terminal display variant was used for experiments involving VHH nanobodies. General growth, transfection, staining, sorting, and data interpretation methods were previously published[6-8]. In brief, singleton dsDNA constructs (IDT gBlocks or eBlocks) or PCR-amplified pooled ssDNA (Twist Bioscience) were cloned into the vector for display. Experiments were conducted on transiently-transfected 293F cells for singleton analysis or via lentiviral transduction of 293F cells after 3-4 days post-transduction for variant pools,

grown in FreeStyle 293 expression medium in either case. Staining either took place with monovalent (TfR-binding CDP or PD-L1-binding CDP work) or tetravalent (VHH nanobody or EGF variant work) protocols, with binder concentrations varying depending on the assay: 100 nM for diversity library screening (Primary EGF Rosetta variant library), 20-100 nM for maturation (EGFd1.5 affinity maturation, VHH nanobody His-doped variant library, PD-L1 binder pH maturation), and 10-50 nM for singleton validation stains. Testing for pH-dependent release involved the conventional staining protocols, but after target protein incubation, cells were pelleted and resuspended in cold pH 7.4 PBS or pH 5.5 citrate-phosphate saline buffer for 5 mins, followed by pelleting at 500xg for 5 mins (combined 10 mins incubation). Cells were then resuspended in buffer for the next step (fluorescent co-stain for monovalent staining protocols, Flow Buffer [PBS with 0.5% bovine serum albumin and 2 mM EDTA] for tetravalent staining protocols). Flow cytometry took place on Becton Dickson FACSAria III or on Sony SH800S instrumentation.

Cancer cell line and primary keratinocyte surface protein flow cytometry

Cell lines were grown by conventional adherent cell culture in 37°C, 5% CO_2 humidified incubators using DMEM + 10% FBS and 1x antibiotic/antimycotic (293T-EGFR-GFP, MDA-MB-231-PD-L1-GFP, A431), RPMI + 10% FBS and 1x antibiotic/antimycotic (A549, H1975, H1650, H1650-PD-L1-GFP, H358), or vendor-recommended growth media for primary keratinocytes (Dermal Cell Basal Medium [ATCC PCS-200-030] and keratinocyte growth kit [ATCC PCS-200-040]). Cells were lifted by removing media, rinsing with room temperature PBS, and incubating with TrypLE Express (ThermoFisher 12605036) until detachment. For staining, following detachment, enzyme was inhibited with complete culture medium, and cells were pelleted at 500xg for 5 min. Cells were resuspended in cold Flow Buffer; for surface EGFR or TfR quantitation, the buffer contained either 10 nM primary antibody (either conjugated with Alexa Fluor 647 [anti-TfR] or pre-labeled with Zenon labeling kit according to manufacturer's instructions [anti-EGFR]) or an equivalent volume of a mock labeling reaction (using Zenon labeling kit reagents but with flow buffer in place of primary antibody); for surface CYpHER detection, Zenon human IgG detection reagent was added as if it were a primary antibody to 10 nM. Cells were incubated in this staining solution on ice for 30 mins, pelleted at 500xg for 5 mins, and resuspended in fresh, cold Flow Buffer containing 1 μg/mL DAPI immediately prior to flow analysis. An example of the gating strategy is found in Supplementary Fig. 18.

Quantitation of protein copies per cell used this same staining protocol, but staining was done alongside Simply Cellular anti-mouse IgG microspheres (Bangs Laboratories 810), with the lot comprised of beads with an average capacity of 73,000 antibodies. For surface quantitation, fluorescence levels of stained cells were compared to that of the IgG microspheres stained in parallel (subtracting values of cells or beads stained without primary antibody), multiplying the cell lines' average fold-difference vs the IgG microsphere fluorescence by 73,000 to arrive at the protein copies per cell.

Catalytic soluble protein uptake

Cells were grown in 24 well plates at 500 µL media per well. For step 1 (CYpHER pre-treatment), cell culture media containing 200 nM recombinant biotinylated target protein ectodomain (EGFRvIII or PD-L1) and 200 nM iFluor 488-conjugated sAvPhire monovalent streptavidin (only 647 channel was analyzed, so this is considered an "unlabeled" stain but used to ensure equivalent target behavior) with or without 50 nM CYpHER were prepared at least 30 min before use, enough for >50 µL per well. 50 µL of this solution was then added to cells growing in 450 µL fresh media, with final concentrations of 20 nM total target protein/streptavidin complex and 5 nM target/streptavidin-saturated binding moieties on CYpHER molecules. Under these conditions, for CYpHER-inclusive conditions, CYpHER molecules saturated with target protein bind to cells and begin cycling through endosomes, trafficking with TfR. After 2 hours, media was removed and cells were gently rinsed twice with PBS before 450 µL fresh media is added. For step 2 (catalytic uptake), cell culture media containing 100 nM recombinant biotinylated target protein ectodomain (EGFRvIII or PD-L1) and 100 nM iFluor 647-conjugated sAvPhire monovalent streptavidin was prepared alongside the step 1 buffers above. 50 µL of this solution was then added to each well for a final concentration of 10 nM target protein/streptavidin complex. Cells were incubated for 24 hrs, during which time cells exposed previously to target/streptavidin-saturated CYpHER that has cycled through the cell and released the target could use the available CYpHER molecules for target binding and uptake. After 24 hrs, cells were rinsed and lifted as above for flow analysis (which included no cell staining, apart from resuspension in Flow Buffer containing 1 µg/mL DAPI). The 647 channel was used for quantitating target uptake.

Surface Plasmon Resonance (SPR) Interaction Analyses

SPR experiments were performed at 25°C on a Biacore 3000 instrument (Cytiva) with a CM3 sensor chip and 10 mM Hepes, pH 7.4 or 5.8, 150 mM NaCl, 3 mM EDTA, 0.05% Surfactant P20, and 0.1 mg/mL BSA as the running buffer. Goat anti-human IgG capture antibody (Jackson ImmunoResearch Laboratories, Inc., West Grove, PA; 109-005-098) was immobilized to flow cells of the sensor chip using standard amine coupling chemistry to a level of 3,800 RU to 3,900 RU. Fc fusion molecules were captured to a level of 70 RU (pH-dependent release VHH) and 55 RU (high affinity at low pH VHH). EGFR concentration ranges were 150 nM to 1.85 nM (pH-dependent release VHH Fc fusion) or 50 nM to 0.617 nM (high affinity at low pH VHH Fc fusion). Each analyte concentration series was run in duplicate and in mixed order, as a means of assessing the reproducibility of binding and managing potential systematic bias to the order of injection. Multiple blank (buffer) injections were run and used to assess and subtract system artifacts. The association phases were monitored for 240 s and the dissociation phases were collected for 600 s, at a flow rate of 30 µL/min. The surface was regenerated with 10 mM glycine, pH 1.5 for 30 s, at a flow rate of 30 µL/min. The data were aligned, double referenced, and fit using Scrubber v2.0 software (BioLogic Software Pty Ltd, Campbell, Australia), which is an SPR data processing and non-linear least squares regression fitting program. The 240 s association phase data and the 600 s dissociation phase data were globally fit to the 1:1 binding model, to determine the kinetic parameters.

Microscopy

Fluorescent cell images were taken on an EVOS M5000 equipped with DAPI (Ex 357/44, Em 447/60), GFP (Ex 470/22, Em 525/50), Texas Red (Ex 585/29, Em 628/32), and Cy7 (Ex 716/40, Em 794/32) cubes. All images within a given experiment were taken with the same light / exposure / gain settings. Image processing took place in ImageJ2 with the Fiji package. When used, background subtraction, contrast enhancement, and gaussian blur filtration (to reduce pixelation) were always done identically between all images within a given experiment using scripts to ensure consistency, maintaining a linear LUT that covers the full range of the image. CT-1212-1 labeling with DyLight 755 labeling kit (ThermoFisher 84539) was as per manufacturer's protocol.

Western blotting

Lysates were prepared with RIPA buffer (ThermoFisher 89900) containing protease/phosphatase inhibitors (Pierce A32959, 1 tablet per 10 mL) and nuclease to reduce viscosity (Pierce 88701, used at 1:1000). Proteins were quantitated by BCA assay (Pierce 23225). SDS-PAGE (4-12% Bis-Tris 1 mm thickness, ThermoFisher NP0321BOX or NP0323BOX) was run with MES buffer (ThermoFisher NP0002) at 180V for 50 min. Gels were transferred to PVDF membrane via iBlot system (ThermoFisher IB401031) on pre-set Program 3. Blotting took place with the LI-COR system (LI-COR 927-66003 [TBS-based blocking and diluent buffers] and ThermoFisher 28360 TBS-Tween 20 wash buffer) for imaging on a LI-COR Odyssey instrument. Primary antibody concentrations were 1:1500 (total EGFR) or 1:3000 (phospho-Y1068 EGFR; actin). Secondary antibody concentrations were 1:15,000. Note: quantitation of bands with bubbles (e.g., Fig. 8D) involved quantitating the unobstructed portion of the band, calibrating against the same portions of the Vehicle bands, and extrapolating.

Cell viability dose response

Cells were passaged into 96 well plates at 500 or 1000 cells/well, with amounts determined by cell titration to produce final confluence of 30-50% in vehicle treatment. 1 day after plating, wells were dosed with vehicle or compound at indicated concentrations (from 10x stocks prepared separately) in technical triplicate. Cells were grown for 4 days (A431 cells) or 7 days (all others) and then viability assessed by CellTiter-Glo 2.0 per manufacturer's instructions. Luminescence data were processed in GraphPad Prism v10, normalized to vehicle (and with vehicle used in curve fits as 0.001 nM), and EC50 values are calculated via log-transformed asymmetric sigmoidal (5PL) curve fit with the following deviations from default settings: Max iterations = 10,000, weighing method = weigh by $1/Y^2$, constrain S > 0, constrain Hill Slope < 0, constrain top < 110%, constrain bottom > 0%.

Immunohistochemistry

Immunohistochemistry was performed by the Fred Hutchinson Cancer Center Experimental Histopathology shared resource (NIH grant P30 CA015704). Paraffin sections were cut at 4 μm, air dried at room temperature overnight, and baked at 60°C for 1 hr. Slides were stained on a Leica BOND Rx autostainer (Leica, Buffalo Grove, IL) using Leica Bond reagents. Endogenous peroxidase was blocked with 3% hydrogen

peroxide for 5 min followed by protein blocking with TCT buffer (0.05M Tris, 0.15M NaCl, 0.25% Casein, 0.1% Tween 20, and 0.05% Proclin 300 at pH 7.6 ± 0.1) for 10 min. Primary antibodies were incubated for 1 hr and polymers were applied for 12 mins, followed by Mixed Refine DAB (Leica DS9800) for 10 min and counterstained with Refine Hematoxylin (Leica DS9800) for 4 min after which slides were dehydrated, cleared and coverslipped with permanent mounting media. IHC antibodies: rabbit anti-EGFR (clone SP84, Cell Marque #14R-15) at 1:25 and mouse anti-Ki67 (clone MIB1, Dako #M7240) at 1:50 with ME Kit, a flexible mouse-on-mouse immunohistochemical staining technique adaptable to biotin-free reagents, immunofluorescence, and multiple antibody staining (https://pubmed.ncbi.nlm.nih.gov/24152994/). Secondary polymer was Power Vision Rabbit HRP Polymer.

CYpHER ELISA

Goat anti-human Fab'(2) (Jackson ImmunoResearch 109-006-190) was used to coat black Maxisorp plates (Thermo 437111) at 500 ng/mL in 100 µL/well incubated overnight, up to 3 days. After coating, all steps were performed at room temperature with extreme care to ensure all wells of a plate were exposed to the same environmental temperature, avoiding gradients across the plates. Wells were aspirated and blocked with 200 µL PBS containing 3% BSA and 0.1% Tween 20 for 2 hr. After aspiration and three rinses with 250 µL/well PBS containing 0.05% Tween 20, samples and standards were applied. For standards, a ten-point standard curve, covering final in-plate concentrations from 300 ng/mL to 0.015 ng/mL, was prepared for each plate using normal mouse serum as diluent. Each sample and standard were then diluted 1:100 (samples and standards) or 1:1000 (samples only as additional dilution series) into Diluent Buffer (PBS containing 1% BSA and 0.1% Tween 20) prior to addition to the plate and allowed to equilibrate to room temperature. Samples were added to the blocked, rinsed plate (100 µL/well) and incubated for 1 hr. After rinsing as above, wells were then incubated with 100 µL mouse anti-human (clone JDC-10, Abcam ab99760) at 50 ng/mL in Diluent Buffer for 1 hr. After rinsing as above, wells were then incubated with 100 µL polyHRP streptavidin (Pierce N200) at 1:20,000 dilution in Diluent Buffer for 1 hr. After rinsing as above, wells were then incubated with 100 µL QuantaBlu Fluorogenic substrate (Pierce 15169), prepared as per manufacturer's recommendation, for 20 min, after which 100 µL of the included Stop solution was added to each well. Plates were then read on a SpectraMax iD3 in top-read fluorescent mode at Ex 325, Em 420. Internal SpectraMax software was used to interpolate the

in-well concentrations for each sample, which was exported for PK analysis. Molecules exhibited a normal biphasic distribution curve, and as such, PK parameters were determined by non-compartmental analysis for IV bolus dosing using Microsoft Excel with the PKSolver 2.0 package.

Supplementary References

1. Ogiso, H. *et al.* Crystal Structure of the Complex of Human Epidermal Growth Factor and Receptor Extracellular Domains. *Cell* **110**, 775–787 (2002).
2. Fleishman, S. J. *et al.* RosettaScripts: A Scripting Language Interface to the Rosetta Macromolecular Modeling Suite. *PLoS ONE* **6**, e20161 (2011).
3. Tyka, M. D. *et al.* Alternate States of Proteins Revealed by Detailed Energy Landscape Mapping. *Journal of Molecular Biology* **405**, 607–618 (2011).
4. Leaver-Fay, A. *et al.* Rosetta3. in *Methods in Enzymology* vol. 487 545–574 (Elsevier, 2011).
5. French, A. R., Tadaki, D. K., Niyogi, S. K. & Lauffenburger, D. A. Intracellular Trafficking of Epidermal Growth Factor Family Ligands Is Directly Influenced by the pH Sensitivity of the Receptor/Ligand Interaction. *Journal of Biological Chemistry* **270**, 4334–4340 (1995).
6. Crook, Z. R., Sevilla, G. P., Mhyre, A. J. & Olson, J. M. Mammalian Surface Display Screening of Diverse Cystine-Dense Peptide Libraries for Difficult-to-Drug Targets. in *Genotype Phenotype Coupling* (eds. Zielonka, S. & Krah, S.) vol. 2070 363–396 (Springer US, New York, NY, 2020).
7. Crook, Z. R. *et al.* Mammalian display screening of diverse cystine-dense peptides for difficult to drug targets. *Nat Commun* **8**, 2244 (2017).
8. Crook, Z. R. *et al.* A TfR-Binding Cystine-Dense Peptide Promotes Blood–Brain Barrier Penetration of Bioactive Molecules. *Journal of Molecular Biology* **432**, 3989–4009 (2020).

Supplementary Figures

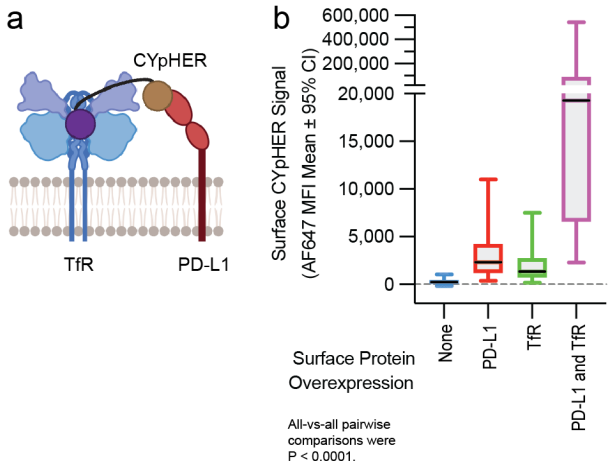

Supplementary Fig. 1. Prototype PD-L1-binding CYpHER binds both TfR and PD-L1 on cells. a Illustration of prototype CYpHER binding both TfR and PD-L1 on a cell surface. **b** 293T cells transfected with either TfR-RFP alone ("None" were RFP[-], "TfR" were RFP[+]) or both TfR-RFP and PD-L1-GFP ("PD-L1" were GFP[+]/RFP[-], "PD-L1 and TfR" were GFP[+]/RFP[+]) were incubated with 10 nM 6xHis-tagged prototype PD-L1 CYpHER for 24 hr and then stained with Alexa Fluor 647 (AF647)-conjugated anti-His. Average AF647 anti-His signals among cells overexpressing one, the other, both, or neither of TfR and PD-L1 are shown. Mean AF647 per cell ± 95% confidence interval (N cells): None, 346 ± 32 (4994); PD-L1, 3601 ± 209 (1850); TfR, 2424 ± 246 (3008); PD-L1 and TfR, 102302 ± 7985 (2550). Experiment in **b** was performed once. All box plots (**b**) feature a median (black line), 25th and 75th percentiles (box boundaries), and 5th and 95th percentiles (whiskers). See the Supplementary Data for full statistical breakdown. Source data are provided as a Source Data file.

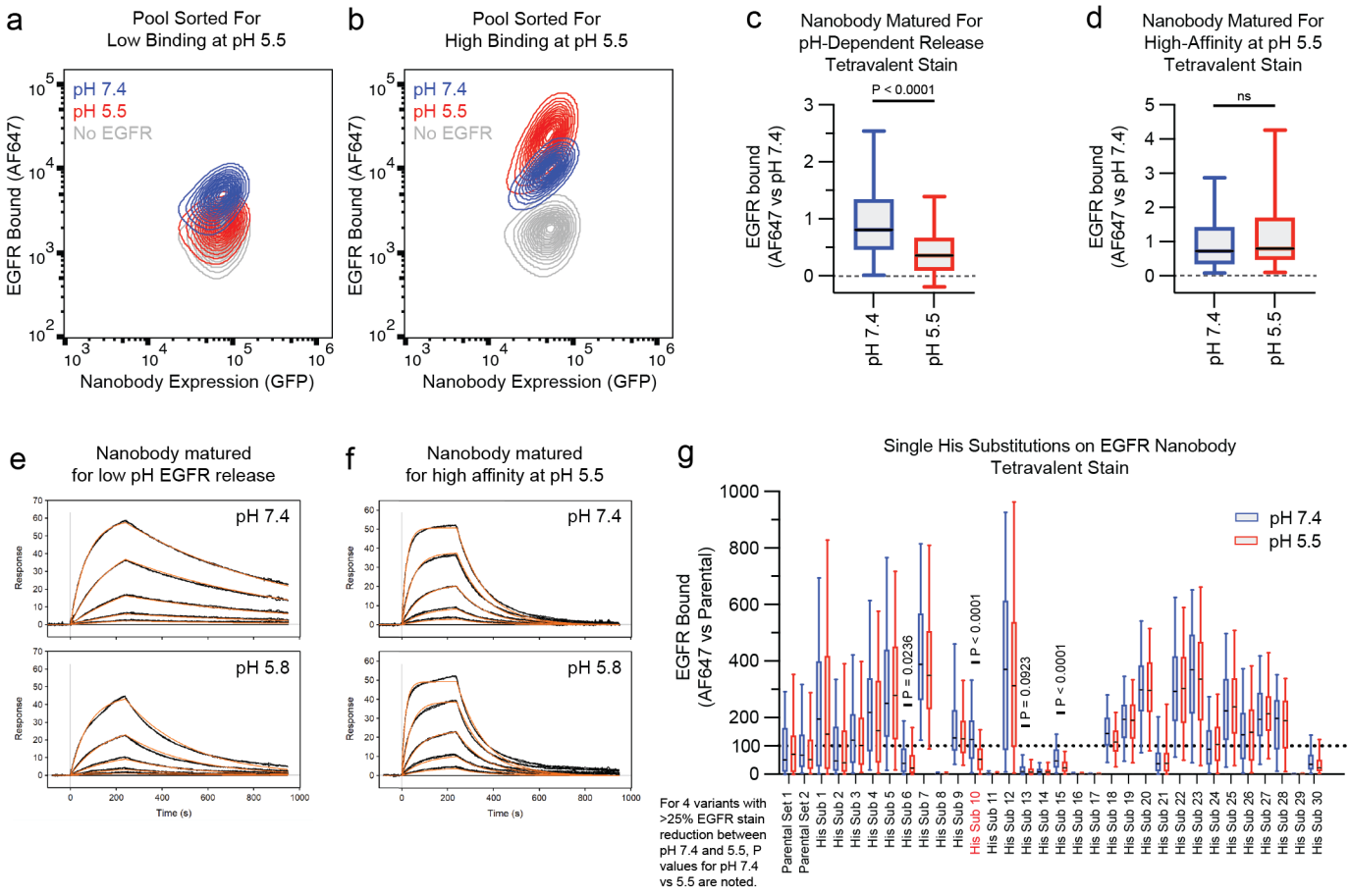

Supplementary Fig. 2. Engineering an EGFR-binding VHH nanobody for pH-dependent release. **a** and **b** Surface display of nanobody and stain with biotinylated EGFR and Alexa Fluor 647 (AF647)-conjugated streptavidin followed by rinse at pH 7.4 (high binding, two rounds) or pH 5.5 (low binding, two rounds), enriched for candidates with pH-dependent release. The final round of sorting at pH 5.5 was split into two populations: low binding (**a**), or high binding (**b**). Shown are the flow profiles of nanobody-displaying cells (nanobody fused to an intracellular GFP), with GFP signal (x axis) and AF647 EGFR (y axis) shown. N cells: pH 7.4, 6844; pH 5.5, 7410; No EGFR, 6644. **c** and **d** The dominant nanobody variants in the populations from **a** and **b** were stained with biotinylated EGFR and AF647 streptavidin followed by pH 7.4 or pH 5.5 rinse. The variant (**c**) from the pH 5.5 low-binding cells (**a**) lost stain in pH 5.5 vs pH 7.4, while the variant (**d**) from the pH 5.5 high-binding cells (**b**) had similar binding in both conditions. Mean AF647 per cell ± 95% confidence interval [CI] (N cells): **a**; pH 7.4, 1.00 ± 0.07 (548) pH 5.5, 0.43 ± 0.05 (421). **b**; pH 7.4, 1.00 ± 0.08 (502); pH 5.5, 1.25 ± 0.40 (36). **e** and **f** Fc fusions of both nanobody variants (**e**, low pH release variant; **f**, high affinity at pH 5.5 variant) were tested in surface plasmon resonance for EGFR binding in pH 7.4 (top) or pH 5.8 (bottom) buffers.

g EGFR-binding VHH nanobody was subjected to conventional Histidine scanning, and singleton variants analyzed for binding to biotinylated EGFR + streptavidin followed by pH 7.4 or pH 5.5 rinse. His substitution 10 had the greatest difference in staining and was selected. N cells per sample: Parental Set 1 pH 7.4, 171; Parental Set 1 pH 5.5, 72; Parental Set 2 pH 7.4, 375; Parental Set 2 pH 5.5, 362; His Sub 1 pH 7.4, 238; His Sub 1 pH 5.5, 111; His Sub 2 pH 7.4, 223; His Sub 2 pH 5.5, 287; His Sub 3 pH 7.4, 209; His Sub 3 pH 5.5, 188; His Sub 4 pH 7.4, 188; His Sub 4 pH 5.5, 200; His Sub 5 pH 7.4, 256; His Sub 5 pH 5.5, 261; His Sub 6 pH 7.4, 259; His Sub 6 pH 5.5, 237; His Sub 7 pH 7.4, 262; His Sub 7 pH 5.5, 223; His Sub 8 pH 7.4, 230; His Sub 8 pH 5.5, 253; His Sub 9 pH 7.4, 242; His Sub 9 pH 5.5, 260; His Sub 10 pH 7.4, 419; His Sub 10 pH 5.5, 432; His Sub 11 pH 7.4, 191; His Sub 11 pH 5.5, 232; His Sub 12 pH 7.4, 248; His Sub 12 pH 5.5, 201; His Sub 13 pH 7.4, 270; His Sub 13 pH 5.5, 248; His Sub 14 pH 7.4, 333; His Sub 14 pH 5.5, 341; His Sub 15 pH 7.4, 408; His Sub 15 pH 5.5, 368; His Sub 16 pH 7.4, 472; His Sub 16 pH 5.5, 417; His Sub 17 pH 7.4, 547; His Sub 17 pH 5.5, 523; His Sub 18 pH 7.4, 574; His Sub 18 pH 5.5, 501; His Sub 19 pH 7.4, 385; His Sub 19 pH 5.5, 267; His Sub 20 pH 7.4, 497; His Sub 20 pH 5.5, 423; His Sub 21 pH 7.4, 549; His Sub 21 pH 5.5, 458; His Sub 22 pH 7.4, 448; His Sub 22 pH 5.5, 354; His Sub 23 pH 7.4, 383; His Sub 23 pH 5.5, 408; His Sub 24 pH 7.4, 261; His Sub 24 pH 5.5, 296; His Sub 25 pH 7.4, 613; His Sub 25 pH 5.5, 580; His Sub 26 pH 7.4, 352; His Sub 26 pH 5.5, 391; His Sub 27 pH 7.4, 276; His Sub 27 pH 5.5, 289; His Sub 28 pH 7.4, 247; His Sub 28 pH 5.5, 280; His Sub 29 pH 7.4, 379; His Sub 29 pH 5.5, 429; His Sub 30 pH 7.4, 381; His Sub 30 pH 5.5, 361. Experiments were performed once. Variants of Interest were defined as those that retained >10% of Parental EGFR binding at pH 7.4 as well as having lost >25% of EGFR binding at pH 5.5 compared to pH 7.4. For each Variant of Interest (His subs 6, 10, 13, and 15), significance was compared between pH 7.4 and pH 5.5 samples by pairwise two-tailed Kolmogorov-Smirnov test. His sub 6 was $P = 0.0236$ between pH 7.4 and pH 5.5; His sub 10 was $P < 0.0001$ between pH 7.4 and pH 5.5; His sub 13 trended towards significant with $P = 0.0923$ between pH 7.4 and pH 5.5; and His sub 15 was $P < 0.0001$ between pH 7.4 and pH 5.5. All box plots (**c**, **d**, and **g**) feature a median (black line), 25^{th} and 75^{th} percentiles (box boundaries), and 5^{th} and 95^{th} percentiles (whiskers). See the Supplementary Data for full statistical breakdown. Source data are provided as a Source Data file.

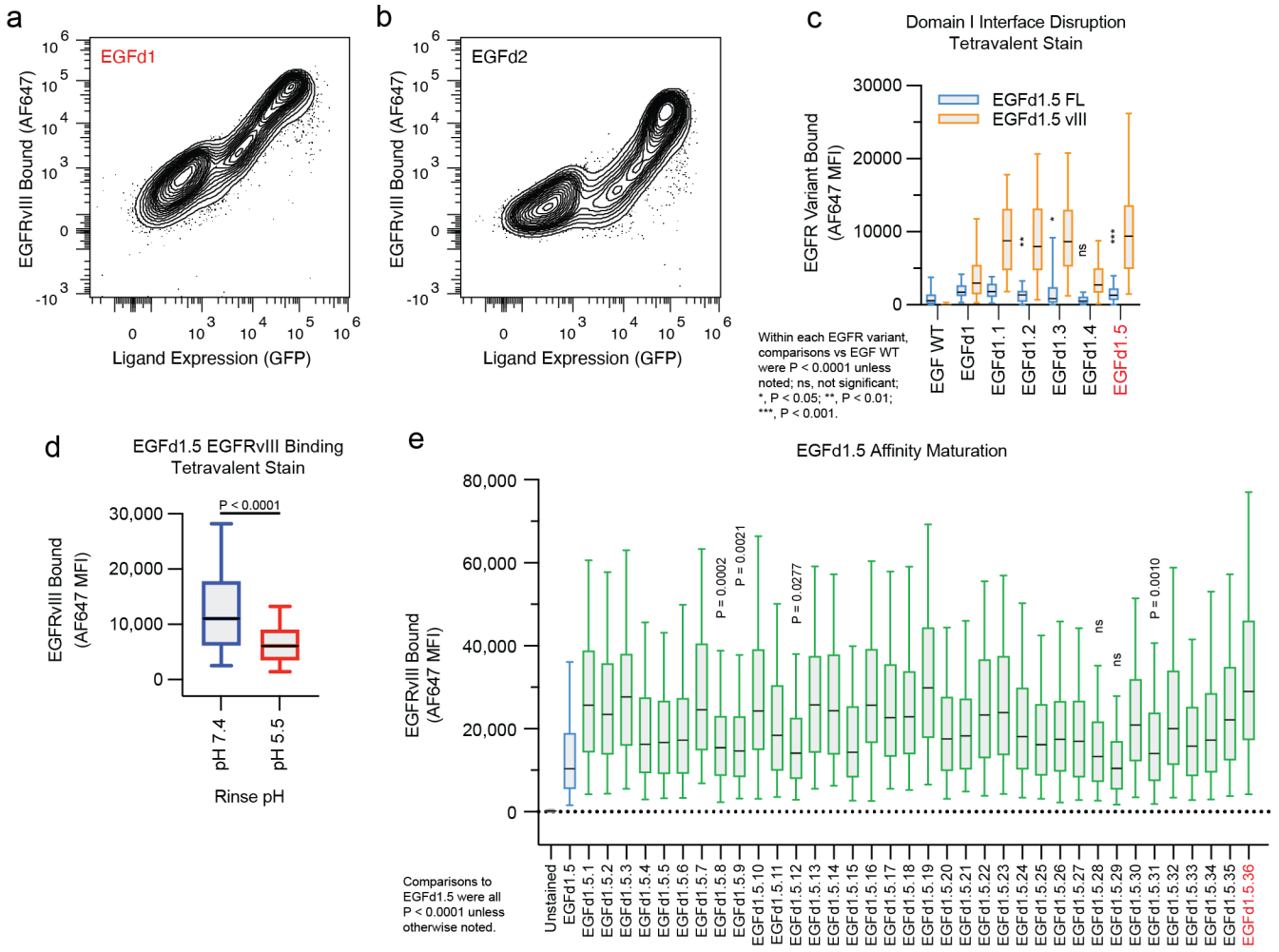

Supplementary Fig. 3. Adapting EGF for use in CYpHER. a and **b** Rosetta protein design was used with an EGF and EGFR co-crystal structure (PDB 1IVO) to design EGF variants with improved predicted binding strength to Domain III. 488 such variants were displayed on 293F cells and stained with biotinylated EGFRvIII and Alexa Fluor 647 (AF647)-conjugated streptavidin. After three rounds of sorting and enrichment for high-AF647-staining cells, singleton candidates were tested for EGFRvIII binding (**a** and **b** showing flow cytometry staining of cells displaying candidates, GFP-fused CDP expression on the x axis, AF647 on the y axis), two of which validated. One (EGFd1) was advanced. N cells: a EGFd1, 7360; b EGFd2, 6986. **c** The interface between EGF and EGFR Domain I was studied, identifying four residues predicted to be key to the interaction. These were mutated to disrupt the interaction, as singletons (EGFd1.1 to EGFd1.4) or all four at once (EGFd1.5). These were surface displayed on 293F cells and stained with biotinylated EGFR (full length or EGFRvIII variant) and AF647-streptavidin, quantitating AF647 per cell by flow cytometry. EGFd1.5 (highest staining with EGFRvIII, low binding to full length EGFR) was advanced. Mean AF647 ± 95% confidence

interval [CI] (N cells): EGF WT FL EGFR, 965 ± 225 (123); EGF WT EGFRvIII, -5 ± 40 (101); EGFd1 FL EGFR, 2020 ± 290 (61); EGFd1 EGFRvIII, 4050 ± 663 (96); EGFd1.1 FL EGFR, 1911 ± 326 (53); EGFd1.1 EGFRvIII, 9220 ± 1571 (43); EGFd1.2 FL EGFR, 1306 ± 216 (84); EGFd1.2 EGFRvIII, 9225 ± 1241 (91); EGFd1.3 FL EGFR, 1981 ± 1198 (33); EGFd1.3 EGFRvIII, 9347 ± 1185 (101); EGFd1.4 FL EGFR, 693 ± 181 (42); EGFd1.4 EGFRvIII, 3476 ± 743 (45); EGFd1.5 FL EGFR, 1523 ± 259 (82); EGFd1.5 EGFRvIII, 10466 ± 1347 (113). **d** EGFd1.5 was tested in surface display for biotinylated EGFRvIII + AF647-streptavidin binding followed by pH 7.4 or pH 5.5 rinse. Remaining AF647 EGFRvIII signal per cell by flow cytometry shown. Mean AF647 ± 95% CI (N cells): pH 7.4, 12697 ± 399 (1553); pH 5.5, 6545 ± 181 (1638). **e** Two rounds of site-saturation mutagenesis affinity maturation of EGFd1.5, followed by combining enriched mutations into 36 variant candidates, yielded binders with improved EGFRvIII binding, shown by flow cytometry per-cell staining with biotinylated EGFRvIII and AF647-streptavidin. EGFd1.5.36 was selected. N cells per sample: Unstained, 419; EGFd1.5, 321; EGFd1.5.1, 298; EGFd1.5.2, 319; EGFd1.5.3, 252; EGFd1.5.4, 450; EGFd1.5.5, 342; EGFd1.5.6, 436; EGFd1.5.7, 430; EGFd1.5.8, 526; EGFd1.5.9, 387; EGFd1.5.10, 390; EGFd1.5.11, 410; EGFd1.5.12, 396; EGFd1.5.13, 448; EGFd1.5.14, 487; EGFd1.5.15, 461; EGFd1.5.16, 315; EGFd1.5.17, 360; EGFd1.5.18, 532; EGFd1.5.19, 454; EGFd1.5.20, 526; EGFd1.5.21, 517; EGFd1.5.22, 440; EGFd1.5.23, 515; EGFd1.5.24, 541; EGFd1.5.25, 553; EGFd1.5.26, 546; EGFd1.5.27, 556; EGFd1.5.28, 536; EGFd1.5.29, 679; EGFd1.5.30, 558; EGFd1.5.31, 629; EGFd1.5.32, 452; EGFd1.5.33, 616; EGFd1.5.34, 481; EGFd1.5.35, 403; EGFd1.5.36, 345. Samples from all 36 variants of EGFd1.5 were compared to EGFd1.5 via Kruskal-Wallis test with Dunn’s correction. All but variants 8, 9, 12, 28, 29, and 31 were $P < 0.0001$ vs EGFd1.5. Variant 8 was $P = 0.0002$ vs EGFd1.5; variant 9 was $P = 0.0021$ vs EGFd1.5; variant 12 was $P = 0.0277$ vs EGFd1.5; variant 28 was not significant vs EGFd1.5 ($P = 0.1540$); variant 29 was not significant vs EGFd1.5 ($P > 0.9999$); and variant 31 was $P = 0.0010$ vs EGFd1.5. Experiments were performed once. See the Supplementary Data for full statistical breakdown. Source data are provided as a Source Data file.

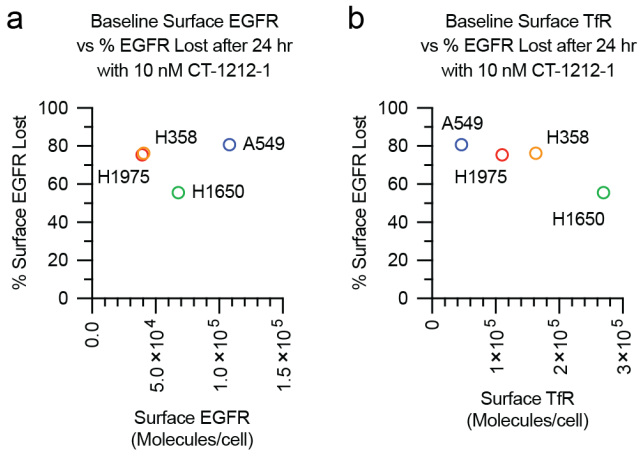

Supplementary Fig. 4. Visualization of baseline surface EGFR and TfR in NSCLC cell lines vs percent surface EGFR lost after 24 hour CYpHER exposure. a and **b** Percent surface EGFR lost in **a** (vs total baseline surface EGFR) and **b** (vs total baseline surface TfR) was calculated by subtracting the 24 hour data in Fig. 4g (Surface EGFR remaining after 10 nM CT-1212-1 treatment) from 100. Baseline total EGFR and TfR is from Fig. 4a.

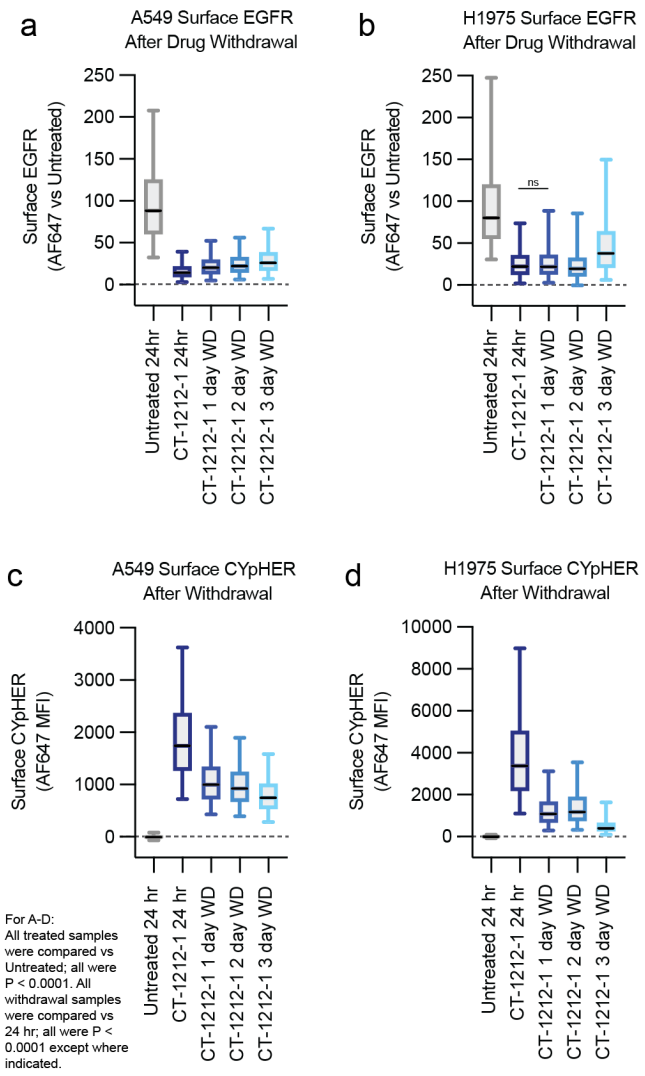

Supplementary Fig. 5. Extended CT-1212-1 withdrawal experiments in A549 and H1975 cell lines. a-d A549 (**a**, **c**) and H1975 (**b**, **d**) cells were untreated or treated with 10 nM CT-1212-1 for 24 hours. In the withdrawal (WD) samples, after 24 hour of CT-1212-1 exposure, media was removed and replaced with fresh media lacking CYpHER, and cells were grown for a further 1, 2, or 3 days (1 day WD, 2 day WD, 3 day WD, respectively). These treatments were staggered so they could be analyzed by flow cytometry at the same time. For **a** and **b**, analysis consisted of staining cells with non-competitive murine anti-EGFR and Alexa Fluor 647 (AF647)-labeled anti-mouse and quantitating stain per cell. For **c** and **d**, analysis consisted of staining cells with AF647-conjugated anti-human Fc and quantitating stain per cell. Mean AF647 ± 95% confidence interval [CI] (N cells) by panel are as follows. **a**: Untreated 24 hr, 100.0 ± 1.8 (3689); CT-1212-1 24 hr, 17.0 ± 0.4 (3559); CT-1212-1 1 day WD, 23.0 ± 0.5 (3639); CT-1212-1 2 day WD, 25.2 ± 0.5 (3778); CT-1212-1 3 day WD, 30.0 ± 0.6 (3708). **b**: Untreated 24 hr, 100.0 ± 3.0 (2164); CT-1212-1 24 hr, 27.7 ± 0.9 (2593); CT-1212-1 1 day WD, 29.6 ± 1.1 (2614); CT-1212-1 2 day WD, 26.8 ± 1.1 (2287); CT-1212-1 3 day WD, 51.7 ± 1.8 (2754).

c: Untreated 24 hr, 0 ± 1 (3612); CT-1212-1 24 hr, 1908 ± 30 (3451); CT-1212-1 1 day WD, 1091 ± 17 (3630); CT-1212-1 2 day WD, 1005 ± 15 (3638); CT-1212-1 3 day WD, 815 ± 13 (3570). **d**: Untreated 24 hr, -1 ± 2 (2333); CT-1212-1 24 hr, 3971 ± 93 (2798); CT-1212-1 1 day WD, 1311 ± 34 (2842); CT-1212-1 2 day WD, 1473 ± 40 (2737); CT-1212-1 3 day WD, 560 ± 19 (2774). Experiments were performed once. See the Supplementary Data for full statistical breakdown. Source data are provided as a Source Data file.

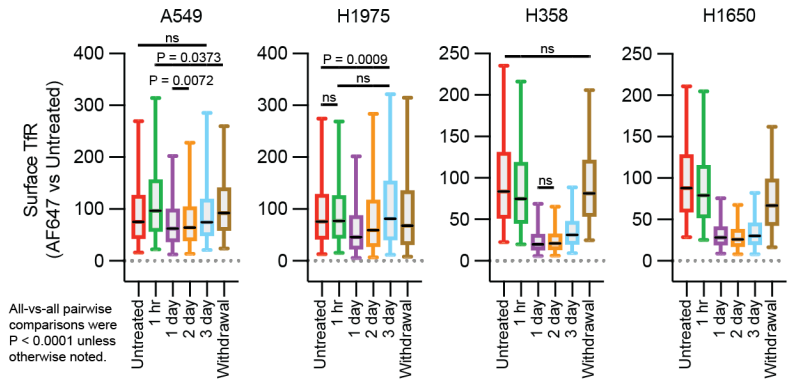

Supplementary Fig. 6. CYpHER effect on surface TfR levels in cancer cell lines. A549, H1975, H358, and H1650 cells untreated or treated with 10 nM CT-1212-1 for 1 hr, 1 day, 2 days, 3 days, or 1 day followed by 1 day without drug ("Withdrawal") and then analyzed by flow cytometry for surface TfR levels by AlexaFluor 647 (AF647)-conjugated anti-TfR, measuring AF647 per cell. Mean AF647 ± 95% confidence interval [CI] (N cells): A549 Untreated, 100.0 ± 2.1 (7872); A549 CT-1212-1 1 hr, 123.5 ± 2.2 (8304); A549 CT-1212-1 1 day, 79.5 ± 1.4 (8739); A549 CT-1212-1 2 days, 84.8 ± 1.6 (8904); A549 CT-1212-1 3 days, 103.0 ± 2.1 (8798); A549 CT-1212-1 Withdrawal, 111.5 ± 1.8 (8321); H1975 Untreated, 100.0 ± 2.3 (5763); H1975 CT-1212-1 1 hr, 99.8 ± 2.5 (4503); H1975 CT-1212-1 1 day, 66.9 ± 1.8 (5890); H1975 CT-1212-1 2 days, 91.3 ± 3.0 (4338); H1975 CT-1212-1 3 days, 114.3 ± 2.8 (6103); H1975 CT-1212-1 Withdrawal, 102.4 ± 3.2 (4396); H358 Untreated, 100.0 ± 1.4 (9035); H358 CT-1212-1 1 hr, 90.8 ± 1.4 (8911); H358 CT-1212-1 1 day, 26.4 ± 0.5 (9001); H358 CT-1212-1 2 days, 26.4 ± 0.5 (8726); H358 CT-1212-1 3 days, 38.1 ± 0.6 (7979); H358 CT-1212-1 Withdrawal, 93.5 ± 1.2 (8199); H1650 Untreated, 100.0 ± 1.3 (7594); H1650 CT-1212-1 1 hr, 91.5 ± 1.3 (7645); H1650 CT-1212-1 1 day, 33.5 ± 0.5 (7788); H1650 CT-1212-1 2 days, 30.4 ± 0.4 (7918); H1650 CT-1212-1 3 days, 36.0 ± 0.5 (8292); H1650 CT-1212-1 Withdrawal, 75.5 ± 1.1 (7627). Within all four cell lines, all samples were compared to one another by Kruskal-Wallis test with Dunn's correction. In A549, Untreated vs 3 day was not significant (P = 0.4123); 1 hr vs withdrawal was P = 0.0373; 1 day vs 2 day was P = 0.0072; and all other comparisons were P < 0.0001. In H1975, Untreated vs 1 hr was not significant (P > 0.9999); Untreated vs 3 day was P = 0.0009; 1 hr vs 3 day was not significant (P = 0.0874); and all other comparisons were P < 0.0001. In H358, Untreated vs withdrawal was not significant (P > 0.9999); 1 day vs 2 day was not significant (P > 0.9999); and all other comparisons were P < 0.0001. In H1650, all comparisons were P < 0.0001.

Experiments were performed once. See the Supplementary Data for full statistical breakdown. Source data are provided as a Source Data file.

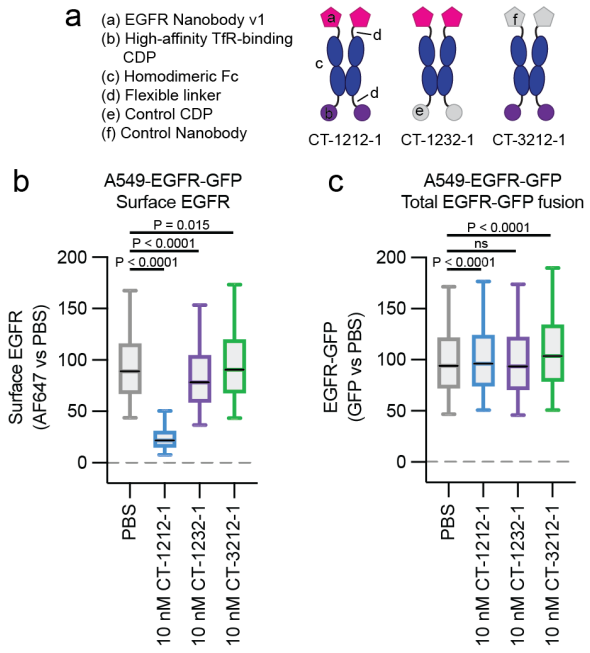

Supplementary Fig. 7. CYpHER- and control-treated A549-EGFR-GFP cells simultaneously quantitated for surface EGFR and total EGFR-GFP. a A549-EGFR-GFP cells were treated for 24 hrs with PBS or 10 nM CT-1212-1, CT-1232-1, or CT-3212-1. **b** and **c** Surface EGFR (**b**), via non-competitive mouse anti-EGFR and Alexa Fluor 647-conjugated anti-mouse, or total EGFR-GFP (**c**), via GFP signal, were quantitated per cell by flow cytometry. Mean AF647 ± 95% confidence interval [CI] (N cells) by panel are as follows. **b**: PBS, 100.0 ± 2.6 (17230); CT-1212-1, 29.3 ± 2.7 (18453); CT-1232-1, 91.4 ± 4.3 (18073); CT-3212-1, 99.4 ± 1.9 (16742). **c**: PBS, 100.0 ± 0.6 (17230); CT-1212-1, 102.7 ± 0.6 (18453); CT-1232-1, 99.8 ± 0.6 (18073); CT-3212-1, 110.0 ± 0.6 (16742). Each treatment was compared to PBS by Kruskal-Wallis test with Dunn's correction. **b**: CT-1212-1 vs PBS was $P < 0.0001$; CT-1232-1 vs PBS was $P < 0.0001$; and PBS vs CT-3212-1 was $P = 0.0150$. **c**: CT-1212-1 vs PBS was $P < 0.0001$; CT-1232-1 vs PBS was not significant ($P = 0.5149$); and PBS vs CT-3212-1 was $P < 0.0001$. Experiment performed once. See the Supplementary Data for full statistical breakdown. Source data are provided as a Source Data file.

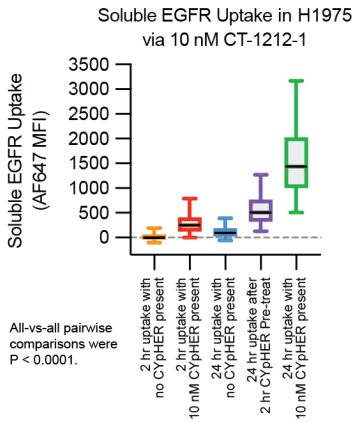

Supplementary Fig. 8. Soluble EGFR uptake with or without CYpHER withdrawal. AlexaFluor 647 (AF647) monovalent streptavidin + biotinylated soluble EGFR uptake after: 2 hr with 10 nM AF647 monovalent streptavidin + biotinylated soluble EGFR but no CYpHER (bar 1); 2 hr with 5 nM CT-1212-1 saturated with AF647 monovalent streptavidin + biotinylated soluble EGFR (bar 2); 24 hr with 10 nM AF647 monovalent streptavidin + biotinylated soluble EGFR but no CYpHER (bar 3); 24 hr incubation with 10 nM AF647 monovalent streptavidin + biotinylated soluble EGFR (but no CYpHER) after 2 hr pre-treatment with 5 nM CT-1212-1 saturated with unlabeled EGFR (bar 4); or 24 hr with 5 nM CT-1212-1 saturated with AF647 monovalent streptavidin + biotinylated soluble EGFR (bar 5). Mean AF647 ± 95% confidence interval [CI] (N cells): 2 hr uptake no CYpHER, 122 ± 4 (5483); 2 hr uptake 10 nM CYpHER, 298 ± 7 (4497); 24 hr uptake no CYpHER, 1587 ± 22 (5708); 24 hr uptake after pre-treat, 579 ± 9 (5778); 24 hr uptake 10 nM CYpHER, 18 ± 3 (3484). All samples were compared to one another by Kruskal-Wallis test with Dunn's correction. All comparisons were $P < 0.0001$. Experiment performed once. See the Supplementary Data for full statistical breakdown. Source data are provided as a Source Data file.

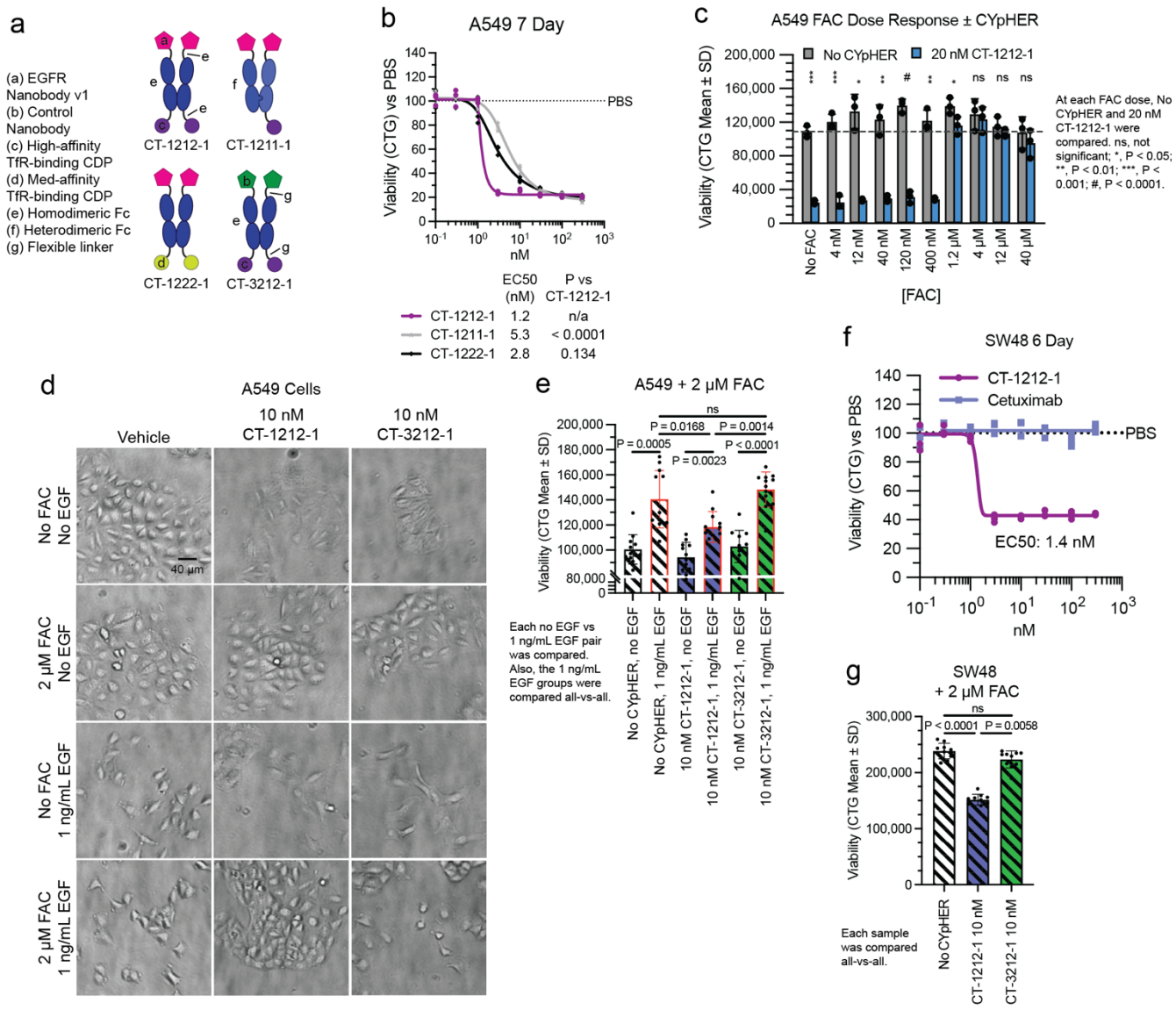

Supplementary Fig. 9. Effects of iron supplementation and EGF on CYpHER-based growth suppression. a Design of EGFR CYpHERs CT-1212-1, CT-1211-1, and CT-1222-1, plus control CT-3212-1 (does not bind EGFR but has the same TfR-binding moiety and avidity as CT-1212-1). **b** Potency of CYpHERs with varying affinity or avidity to TfR in an A549 growth disruption assay. CellTiter-Glo 2.0 [CTG] viability per well shown. N = 3 wells per dose per molecule. EC50 calculated by asymmetric sigmoidal [5PL] curve fit. A549 CT-1212-1 data is the same as presented in Fig. 7g. **c** A549 cells (KRas G12S mutant) were treated with 0 or 20 nM CYpHER, with increasing amounts of ferric ammonium citrate (FAC), a cell-penetrant chelated iron supplement. CTG viability per well shown. N = 3 wells per condition. **d** A549 cells treated with or without 1 ng/mL EGF, 2 µM FAC, 10 nM CT-1212-1, and/or 10 nM CT-3212-1 for 5 days in culture and photographed at 20x objective, bright field phase contrast. Both CT-1212-1 and CT-3212-1 disrupted growth (flat, senescent-like morphology, few cells), which was suppressed by FAC. EGF also induced a migratory phenotype (cells moving

away from one another instead of growing in tight colonies); with FAC present to permit growth, this migratory phenotype is suppressed by EGFR CYpHER (CT-1212-1) but not by the control (CT-3212-1). **e** Effect of EGF (1 ng/mL) on A549 growth, with or without 2 μM FAC, 10 nM CT-1212-1, and/or 10 nM CT-3212-1 for 6 days. CTG viability per well shown. N = 12 wells per condition. **f** Effect of CT-1212-1 and cetuximab on colon cancer cell line SW48 (wild type KRas) after 6 days growth. CTG viability per well shown. **g** Effect of CT-1212-1 and CT-3212-1 on growth of SW48 cells after 6 days in the presence of FAC. CTG viability per well shown. N = 10 wells per condition. Experiments in **b**-**g** performed once. See the Supplementary Data for full statistical breakdown. Source data are provided as a Source Data file.

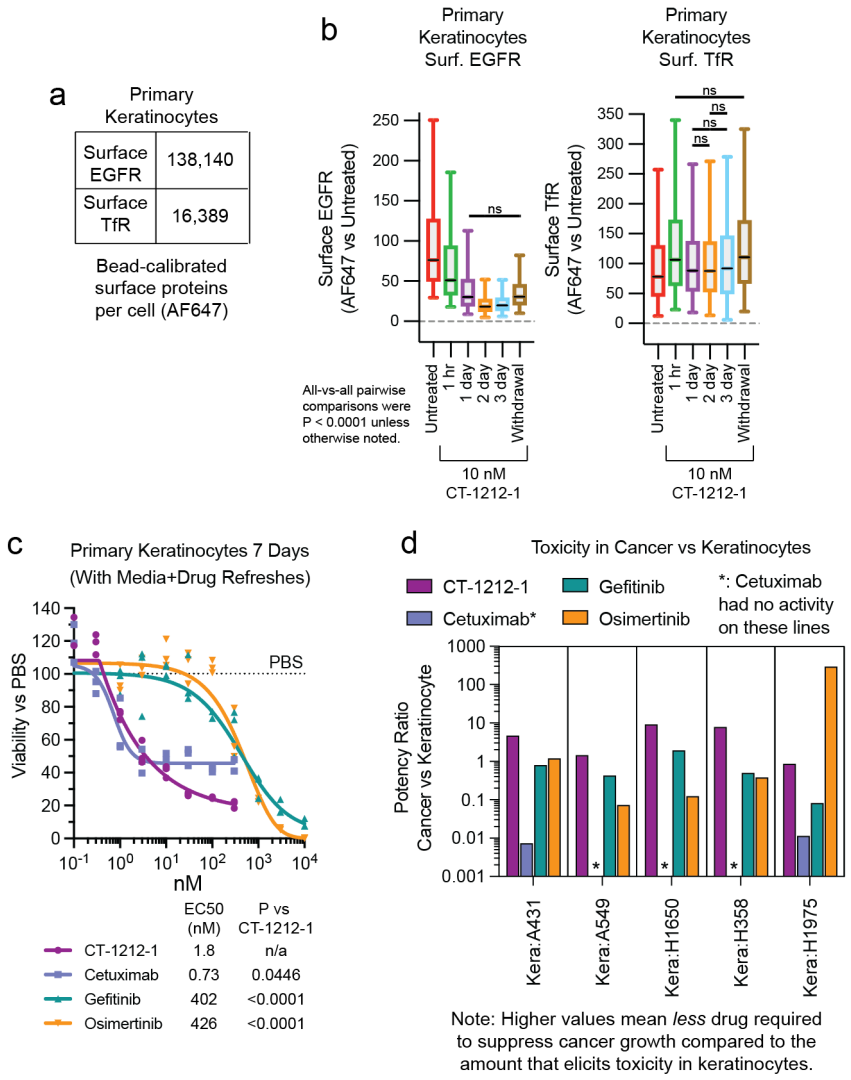

Supplementary Fig. 10. Effect of CYpHER on primary keratinocytes. a Primary human dermal keratinocytes were flow analyzed alongside calibration beads to quantitate surface EGFR and TfR levels. **b** Keratinocytes were untreated or treated with 10 nM CT-1212-1 for 1 hr, 1 day, 2 days, 3 days, or 1 day followed by 1 day without drug ("Withdrawal") and then analyzed by flow cytometry for surface EGFR levels (left) and surface TfR levels (right). N cells per sample as follows. Left (Surface EGFR): Untreated, 8026; CT-1212-1 1 hr, 8197; CT-1212-1 1 day, 8086; CT-1212-1 2 days, 8000; CT-1212-1 3 days, 8120; CT-1212-1 Withdrawal, 8177. Right (Surface TfR): Untreated, 7642; CT-1212-1 1 hr, 7955; CT-1212-1 1 day, 7985; CT-1212-1 2 days, 7688; CT-1212-1 3 days, 7890; CT-1212-1 Withdrawal, 7611. **c** Keratinocytes were treated for 7 days, with a media exchange (including drug refresh) on day 4, with CT-1212-1, cetuximab, gefitinib, or osimertinib. After treatment, cell levels per well were quantitated by CellTiter-Glo 2.0 [CTG] assay. N = 3 wells

per treatment per dose. EC50 calculated by asymmetric sigmoidal [5PL] curve fit. **d** EC50 values of cancer cell lines (Fig. 7i) compared to the EC50 values of the primary keratinocyte treatments. Shown is the single value ratio of keratinocyte EC50 as numerator and cancer line EC50 as denominator. This results in higher values when compound is more potent at suppressing growth of cancer lines relative to effect on keratinocyte growth. Experiments in **a**-**c** performed once. See the Supplementary Data for full statistical breakdown. Source data are provided as a Source Data file.

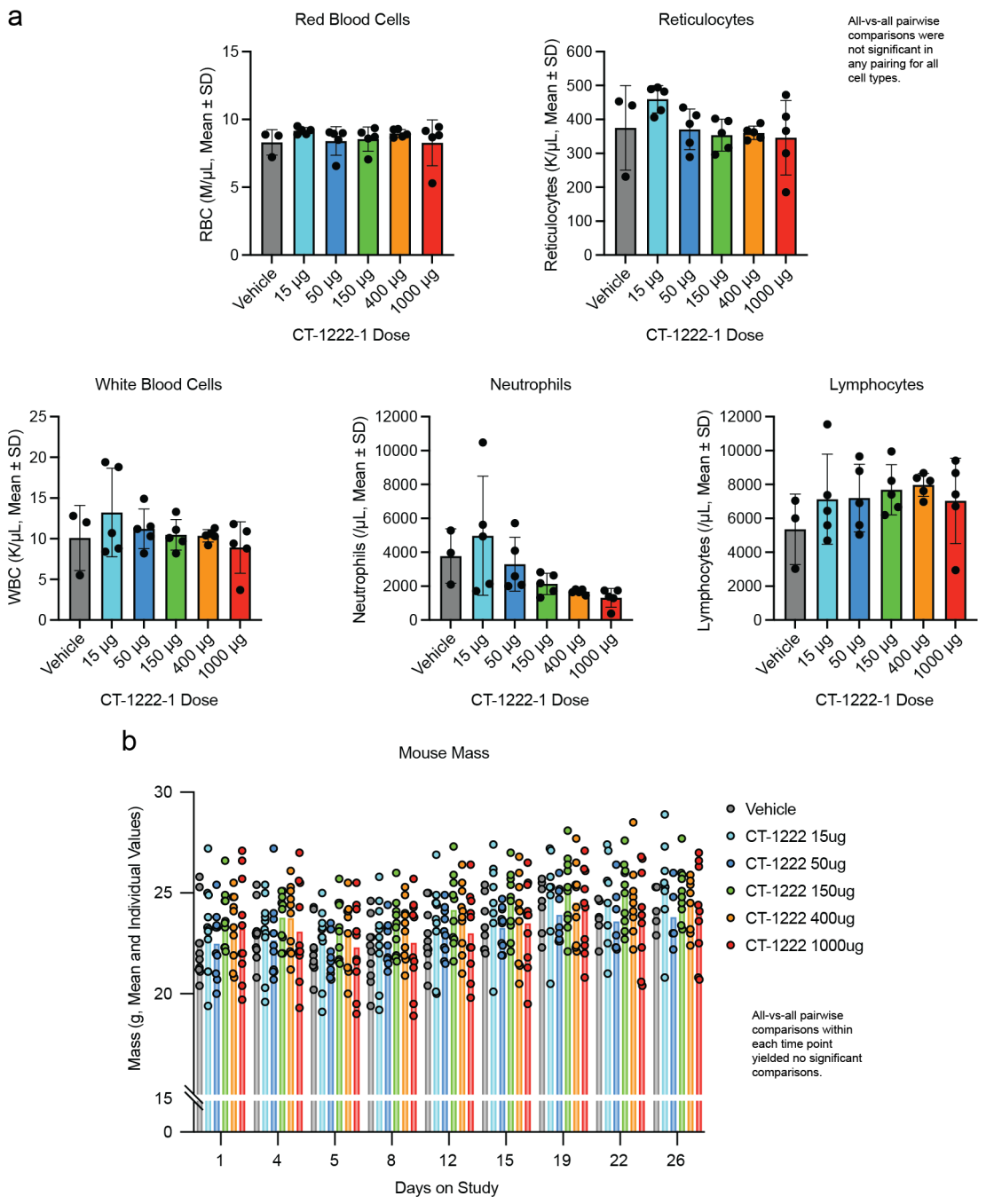

Supplementary Fig. 11. Select blood cell counts and animal mass from chronic CT-1222-1 exposure. Mice were treated twice per week IV with various doses of CT-1212-1 for four weeks. **a** At the end of these four weeks, 48 hours after the final dose, blood was collected for CBC analysis. Values for red blood cells, reticulocytes, white blood cells, neutrophils, and lymphocytes are shown. N = 5 mice for all conditions except vehicle, which was N = 3 mice. Within each blood cell type, counts were compared between all samples (all vs all) via Kruskal-Wallis test with Dunn's correction. No comparisons were found to be significant in any cell type. **b** Animal mass at each timepoint is shown. N (mice) per treatment and time point: Vehicle Day 1, 10; Vehicle

Day 4, 10; Vehicle Day 5, 10; Vehicle Day 8, 10; Vehicle Day 12, 10; Vehicle Day 15, 8; Vehicle Day 19, 7; Vehicle Day 22, 6; Vehicle Day 26, 5; CT-1222-1 15 µg Day 1, 10; CT-1222-1 15 µg Day 4, 10; CT-1222-1 15 µg Day 5, 10; CT-1222-1 15 µg Day 8, 10; CT-1222-1 15 µg Day 12, 10; CT-1222-1 15 µg Day 15, 8; CT-1222-1 15 µg Day 19, 8; CT-1222-1 15 µg Day 22, 8; CT-1222-1 15 µg Day 26, 8; CT-1222-1 50 µg Day 1, 10; CT-1222-1 50 µg Day 4, 10; CT-1222-1 50 µg Day 5, 10; CT-1222-1 50 µg Day 8, 10; CT-1222-1 50 µg Day 12, 10; CT-1222-1 50 µg Day 15, 10; CT-1222-1 50 µg Day 19, 9; CT-1222-1 50 µg Day 22, 7; CT-1222-1 50 µg Day 26, 5; CT-1222-1 150 µg Day 1, 10; CT-1222-1 150 µg Day 4, 10; CT-1222-1 150 µg Day 5, 10; CT-1222-1 150 µg Day 8, 10; CT-1222-1 150 µg Day 12, 10; CT-1222-1 150 µg Day 15, 10; CT-1222-1 150 µg Day 19, 10; CT-1222-1 150 µg Day 22, 10; CT-1222-1 150 µg Day 26, 10; CT-1222-1 400 µg Day 1, 10; CT-1222-1 400 µg Day 4, 10; CT-1222-1 400 µg Day 5, 10; CT-1222-1 400 µg Day 8, 10; CT-1222-1 400 µg Day 12, 10; CT-1222-1 400 µg Day 15, 10; CT-1222-1 400 µg Day 19, 10; CT-1222-1 400 µg Day 22, 9; CT-1222-1 400 µg Day 26, 8; CT-1222-1 1000 µg Day 1, 10; CT-1222-1 1000 µg Day 4, 10; CT-1222-1 1000 µg Day 5, 10; CT-1222-1 1000 µg Day 8, 10; CT-1222-1 1000 µg Day 12, 10; CT-1222-1 1000 µg Day 15, 10; CT-1222-1 1000 µg Day 19, 10; CT-1222-1 1000 µg Day 22, 9; CT-1222-1 1000 µg Day 26, 9. Grouped samples were tested all-vs-all by a two-way mixed-effects model with Tukey correction. Within each time point, there were no significant pairwise comparisons. The smallest P value was at Day 5, 50 µg vs 150 µg ($P = 0.2286$). Experiment performed once. See the Supplementary Data for full statistical breakdown. Source data are provided as a Source Data file.

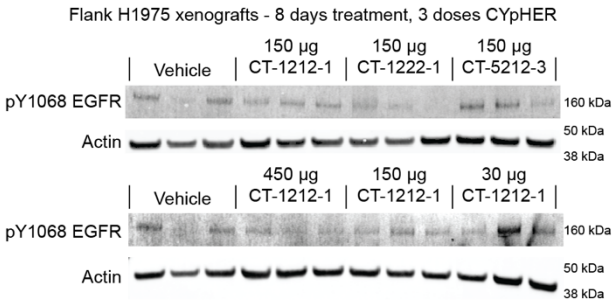

Supplementary Fig. 12. EGFR phosphotyrosine 1068 Western blots from flank tumor samples. Tumor samples match those shown in Fig. 8d. N = 3 mice per condition, all mice shown. Experiment performed once.

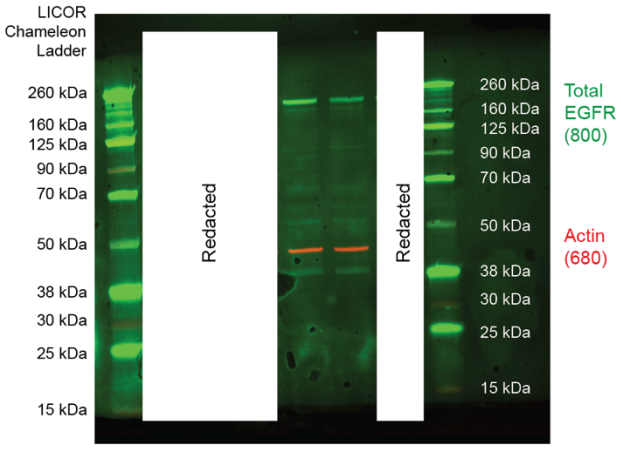

Supplementary Fig. 13. Full Western blot from Fig. 3f.

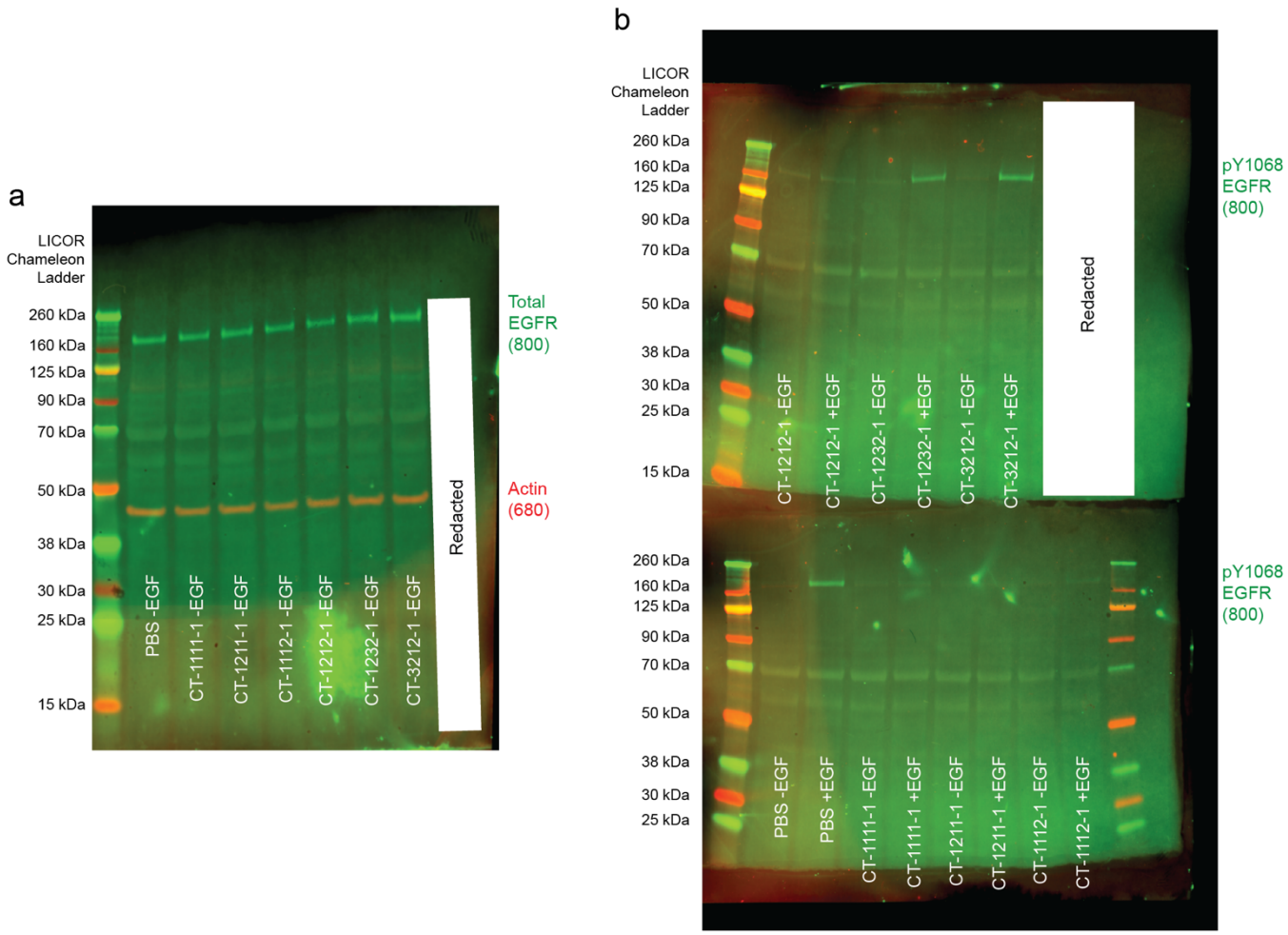

Supplementary Fig. 14. Full Western blot from Fig. 7b.

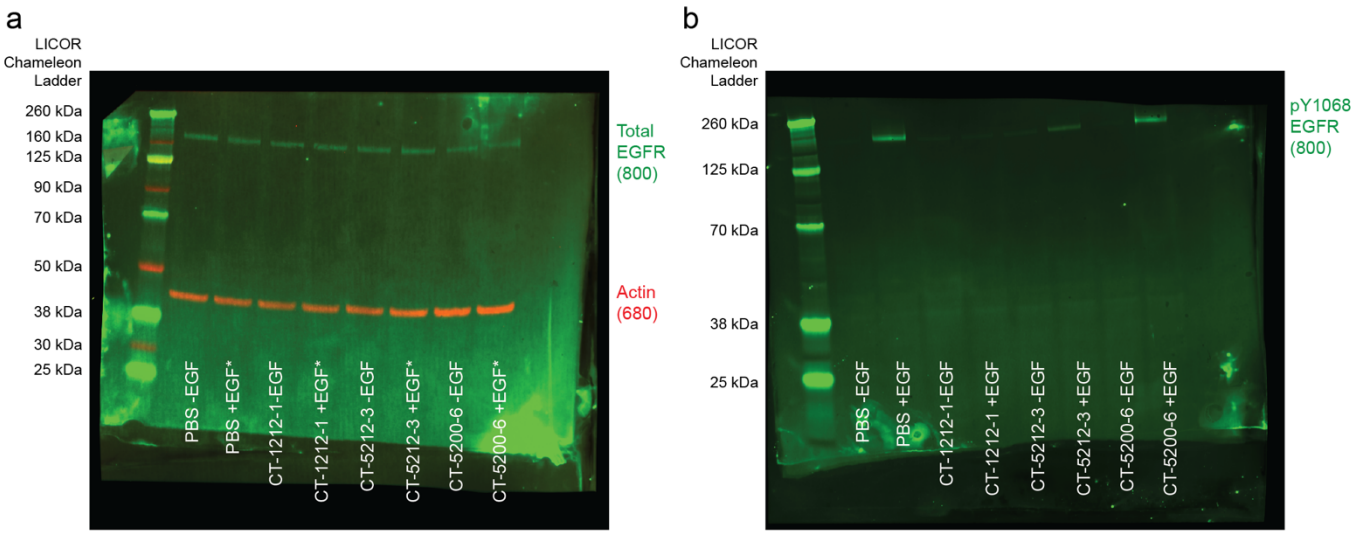

Supplementary Fig. 15. Full Western blot from Fig. 7c. a Total EGFR; lanes in a marked with asterisk were not shown in Fig. 7c. **b** Phosphotyrosine 1068 (pY1068).

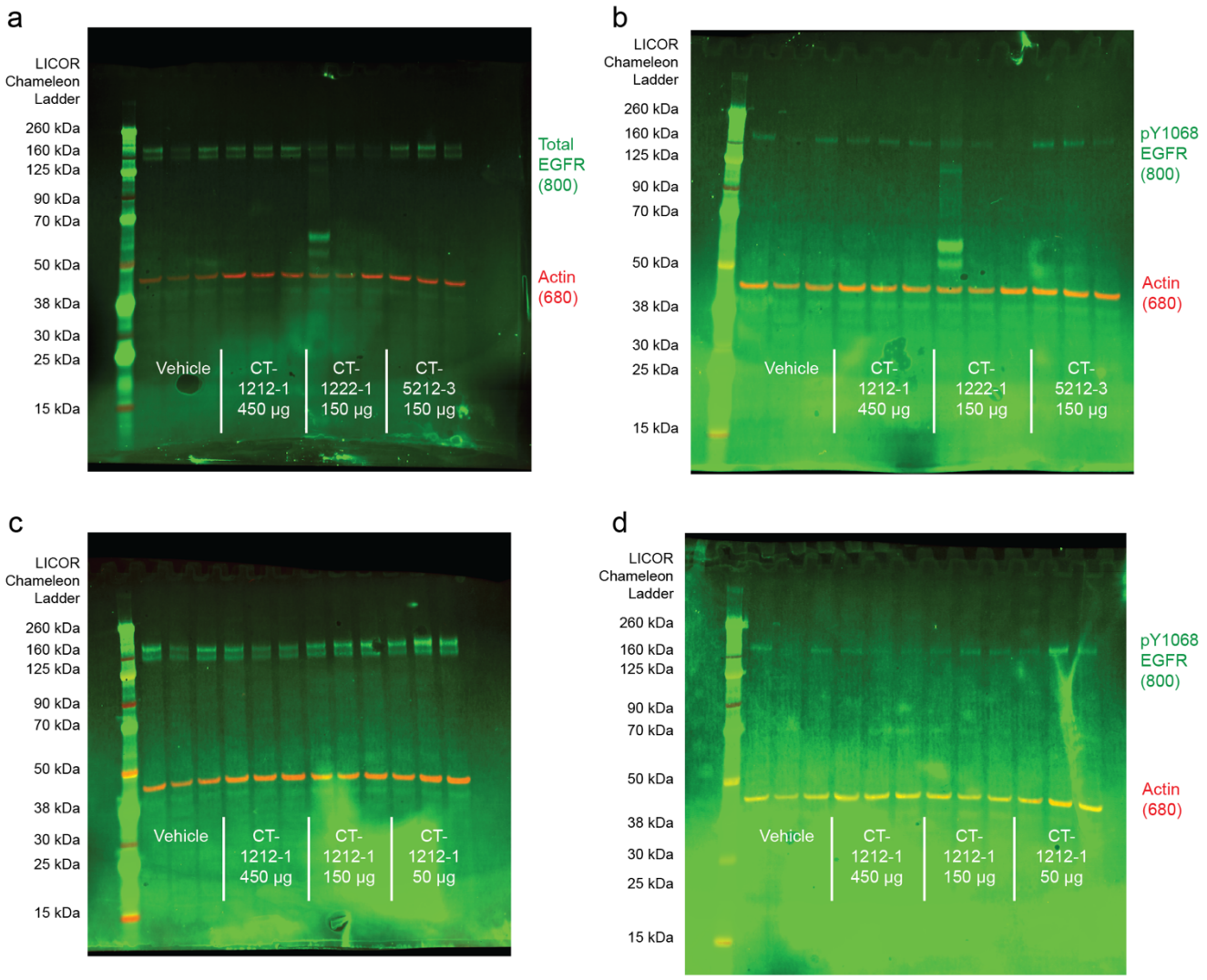

Supplementary Fig. 16. Full Western blots from Fig. 8d and Supplementary Fig. 12. a Fig. 8d top. **b** Fig 8d bottom. **c** Supplementary Fig. 12 top. **d** Supplementary Fig. 12 bottom.

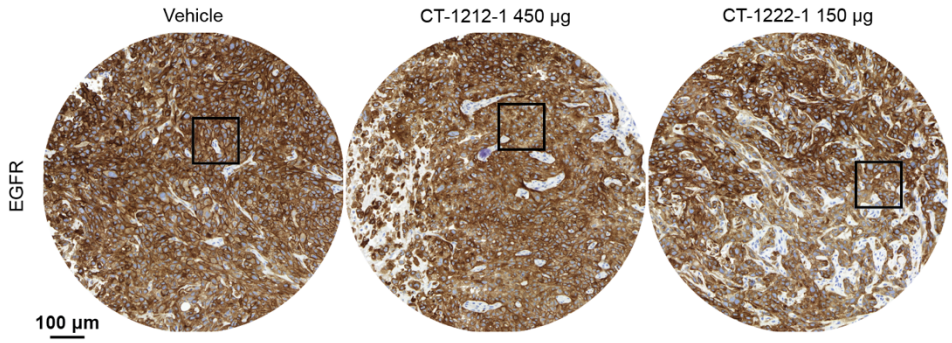

Supplementary Fig. 17. Full fields of EGFR histology shown cropped in Fig. 8f. The bounding boxes identify the crop areas used in Fig. 8f.

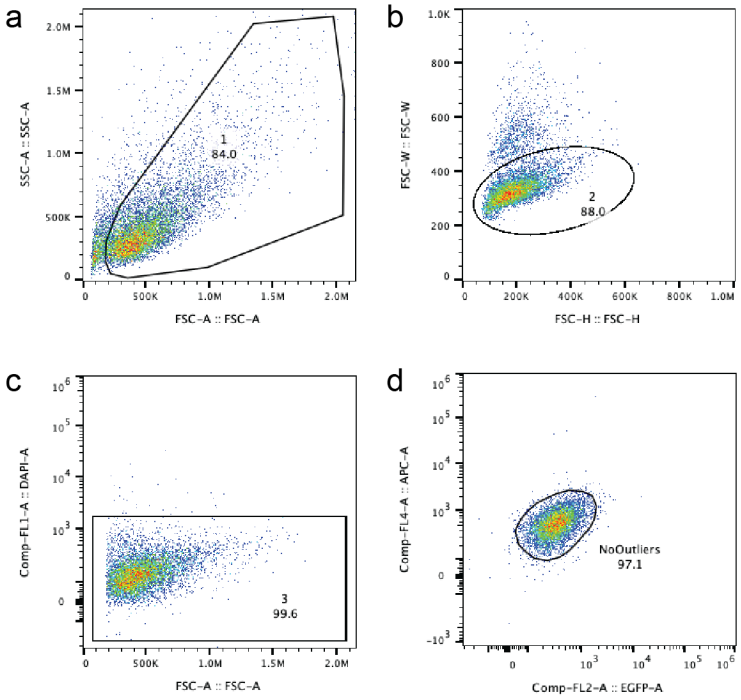

Supplementary Fig. 18. Exemplary flow cytometry gating strategy. a Cells (here, H1650 stained with AlexaFluor647 anti-EGFR) are first gated for forward and side scatter areas (FSC-A, SSC-A) to eliminate debris, which is low in forward scatter vs side scatter. **b** Next, singletons are selected by identifying events within the main field in a FSC-width vs FSC-height (FSC-W, FSC-H). **c** Dead cells that are DAPI+ are next eliminated, gating to only include DAPI- cells. **d** Autofluorescent outliers are finally eliminated by gating to the main cloud of cells in an APC vs GFP fluorescence plot. This successfully removes autofluorescent events whether or not the cells are APC+ or GFP+.